HEFAT2007
5th International Conference on Heat Transfer, Fluid Mechanics and Thermodynamics
Sun City, South Africa
KS3

FINITE ELEMENT ANALYSIS OF MATERIAL FLOW PATTERNS IN FRICTION STIR SPOT WELDING OF AL 6082-T6 USING DIFFERENT PROCESS PARAMETERS AND TOOL GEOMETRIES

S. Khosa, T. Weinberger*, N. Enzinger
*Author for correspondence
JOIN – Network of Excellence for Joining,
Austria
Institute for Materials Science, Welding and Forming (IWS)
Graz University of Technology, Graz, 8010
Austria
E-mail: thomas.weinberger@TUGraz.at

ABSTRACT

From application view point simple looking process of Friction Stir Spot Welding (FSSW) works on a complex thermo-mechanical mechanism. The strong inter-dependency of parameters responsible for heat generation and material flow like friction co-efficient, vertical force, rotational speed, tool geometry & dimensions, shear yield strength, conductivity and heat capacity etc. makes it a challenge to investigate the mechanism for FSSW process. At the start of the process, rigid solid behavior of work piece dominates. As the process proceeds, the rise in temperature due to frictional and deformation heat inputs, softens the material and it is assumed that the material transfer under the tool behaves like that of a fluid. In this part of on going research for FSW at IWS, a thermo-fluid coupled, three dimensional and transient model for quasi–steady state condition during FSSW process, is developed. The effects of different process parameters like tool geometries, rotational speed and dwell time on material flow patterns are studied experimentally and modeled, using general purpose FE software package MSC Marc®. The predicted results of the Finite Element study in terms of fluid velocity profile, nugget size and shape are compared with experimental observations carried out at IWS laboratories of TU Graz.

INTRODUCTION

FSW is a solid state joining process to obtain high quality joints [1]. Heating is provided by the friction and the energy dissipated due to material flow as a result of mechanical work caused by a rotating tool in the work piece. Essential components of the process are shown in figure 01; a rotating tool with vertical load exertion (and transverse travel along the weld line) capability, work piece to be joined, clamping and back plate and the tool fundamentally consists of shoulder and pin parts.

The Friction Stir Spot Welding (FSSW) process may be divided into four main phases, namely, touch down, plunge, dwell and retraction. As the process begins the rotating tool commences touch down and with vertical downward force, frictional heat is generated at the interface between tool pin and work piece.

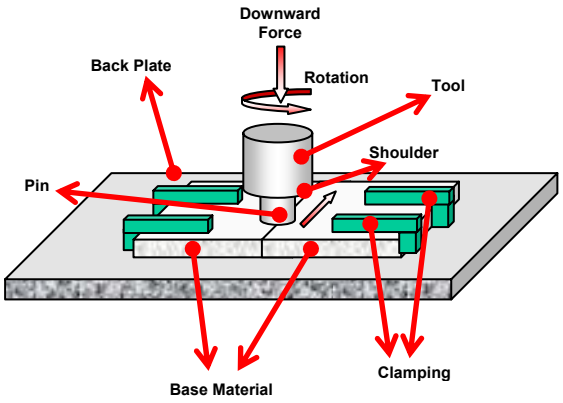

Figure 01: Components of FSW Process

With the rise in temperature, the yield strength of the work piece drops, it starts to soften and the tool pin plunges into the material.

Work piece material around and under the pin experiences extensive deformation during this plunge phase. The energy dissipated due to this deformation adds up the heat input hence giving further rise in temperature and softening of material. At the completion of plunge phase when the tool shoulder touches the upper surface of the work piece, a large amount of frictional heat is generated due to bigger area and high relative linear velocities at broader skirts of the shoulder. It is assumed for this work that heat input during the plunge phase rises the temperature to a level that the yield strength of the material is dropped enough to start a material flow at very low applied stresses i.e. comparable to viscous fluid. Then starts the dwell phase, where the tool position is kept constant to allow a mature nugget development. For FSSW, the dwell phase is directly followed by retraction, as shown in figure 02. Whereas for FSW process the tool is traversed along the weld line before retraction and generally smaller (than that in FSSW process) or no dwell times are allowed, i.e. traverse motion of the tool is started just after the plunge or after small dwell interval.

This apparently simple looking process is governed by complex heat generation and material flow mechanisms. For this relatively new welding technology the consensus about the mechanism is yet to be achieved [2]. Regarding the mechanism of heat generation and

material flow during FSSW, it is hypothized that during the touch down phase, all-slip condition prevails at tool-work piece interface and generates frictional heat.

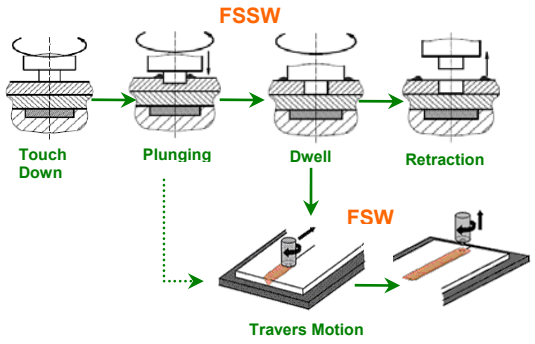

Figure 02: Process steps during FSSW and FSW

As the plunge phase starts the material deformation contributes to heat input by the deformation energy dissipation and further raises the temperature. When the shoulder touches the work piece and adds up a large amount of heat energy by friction at shoulder-work piece interface, the rise in temperature is adequate to make the material soft enough to create sticking condition at that interface. In other words the work piece material behaves like a viscous fluid at the interface. With the domination of sticking condition the heat input due to friction decreases. Also for the deformation lower energy is required at these temperatures. Thus over-all energy input is decreased and hence the temperature. The yield strength of the work piece, that is strongly dependant upon temperature as an inverse proportionality, starts to increase, making the tool-work piece interface conditions to switch back to the slip condition. Then again higher energy input for material deformation is required. This switch over of the slip-stick conditions forms a kind of loop as shown in figure 03. Thus it is clear that the temperature profile of the work piece determines the extent and shape of the volume that will behave like a viscous fluid, around the tool and this process is schematically summarized in figure 04. The extent and shape of volumetric pool which forms the stirred zone of FSSW/FSW weld and the temperature profile further guide the profile of Thermo-Mechanically Affected Zone (TMAZ) and Heat Affected Zone (HAZ). The TMAZ may be considered as a transitional boundary region between pseudo-fluid stirred zone and rigid solid boundary of the work piece [3,7].

To fully understand the mechanism of FSSW/FSW, the main challenges are to determine:

- The over all heat input, its distribution and fractional contribution from friction and deformation phases
- Resulting temperature profile
- Material flow patterns/types and the velocities in the work piece

As experimental observations for above mentioned points are not possible yet to a level that could give a thorough insight into the mechanism, so the mathematical estimations of these aspects of the process are employed [3].

For the work carried out at IWS – TUG, regarding FSSW and FSW mechanism understanding, three dimensional, fully coupled, transient model is being developed. At this stage, a thermo-fluid coupled, transient model for dwell phase during FSSW is compared with the experimental observations of nugget shape and size. The literature regarding the mathematical modeling of FSSW and FSW which came under our review shows studies by thermo-mechanical coupled model [4,6] and also based upon CFD studies [1,5,8] to predict the material flow and thermal fields.

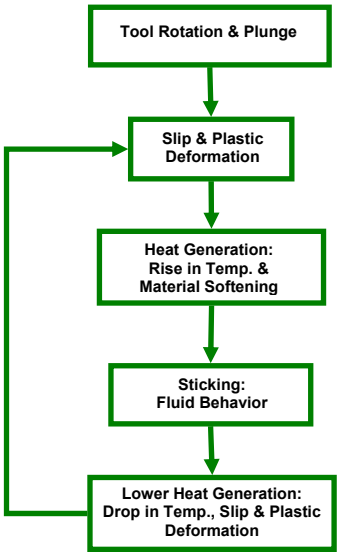

Figure 03: Flow chart for hypothesis of slip-stick loop

The main advantages of considering the material being stirred as a fluid are to predict the fluid velocities and geometrical effects of the tool geometry on material flow. The recent models for material flow and tool design studies follow the CFD approach [5,8]. None of the asserted work which came under our review on material flow during FSSW, reports direct comparison of mathematical model and experimental observations for the effects of different simple tool geometries. This can provide a basic platform to build generalized understanding regarding the mechanism of material flow during FSSW/FSW, process parameter optimization and tool design. So in the current work comparisons of nugget shape and size for observed and modeled results have been attempted.

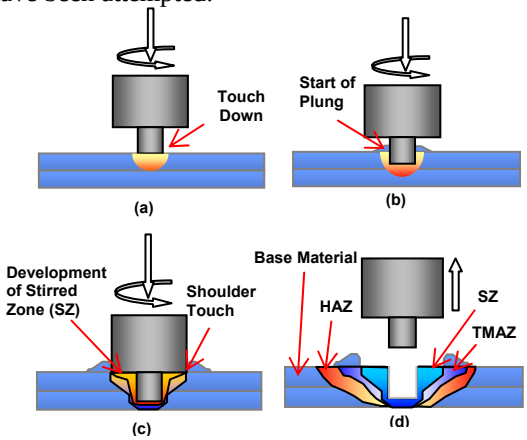

Figure 04: Process schematic for the development of stirred, TMA and HA zones

EXPERIMENTAL DETAILS

The Friction stir spot welds were produced at the friction stir lab at Graz University of Technology using

the MTS I-Stir BR4. This is a FSW portal machine with a tool rotational speed of up to 3200 rpm, a downward force of 35kN and maximum spindle torque of 180Nm. To perform the spot welds, we used three different tools from steel H13 (figure 5). The first tool had no pin. The second tool had cylindrical pin geometry (diameter: 4 mm, pin length: 4 mm). The third tool had tapered pin geometry (diameter: 3.5 to 5 mm, pin length: 4 mm). In all cases the shoulder diameter is 13 mm (Figure 05).

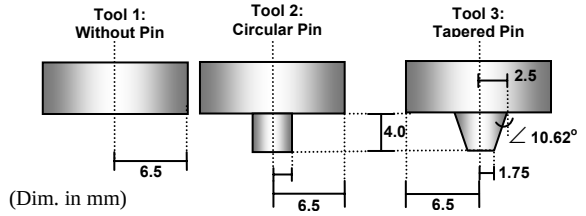

Figure 05: Tool geometries used in the experiments and the model

To perform the spot welds, we used 3mm thick plates of Aluminum AA 6082-T6 with a width of 100mm and a length of 500mm in an overlap joint configuration. The chemical composition of Al6082T6 is shown in table 01.

Table 01: Chemical composition of Al6082-T6

Element	Wt (%)	Element	Wt (%)
Si	0.7-1.3	Cr	0.25
Fe	0.5	Zn	0.2
Cu	0.1	Ti	0.1
Mn	0.4-1	Ga	-
Mg	0.6-1.2	Other	0.15
Ni	-	Al	Balance

The spot welds were produced using a different set of spindle speeds and dwell times. The spindle speed was varied between 800 and 2000 rev/min while the dwell time varied from 0 to 5 sec. The plunge rate was constant with 12 mm/min and the plunge depth was constant. For tool 1 it was 0.15 mm and for tool 2 and 3 it was 4.15 mm. A summary of the parameter sets for each tool is given in table 2.

Table 02: (a) Parameter set for tool-2 experiments & (b) for tool 1 & 3

(2-a)

RPM/Dwell Time (sec)	0	1	3	5
800	x	x	x	x
1200	x	x	x	x
1600	x	x	x	x
2000	x	x	x	x

(2-b)

RPM/Dwell Time (sec)	0	1	3	5
800				
1200		x	x	x
1600				
2000		x	x	x

The forces and torque were measured by high accuracy pressure cells and recorded simultaneously during each spot welding operation. After performing of the spot welds, the samples were prepared for metallographic inspections.

MODEL DESCRIPTION

The model developed in this study is three dimensional, time domain transient, coupled thermo-fluid for the dwell phase of FSSW process using general purpose Finite Element Analysis (FEA) software package MSC Marc®. The main objective of current model under discussion is to gradually increase the complexity associated with the material flow during FSSW, so the simplest possible model is developed and compared with the simple tool geometries i.e. with-out threads and other features. The model consists of three materials i.e. tool, work piece and back plate. Mesh for tool and work piece for tool-2 & 3 are shown in figure 06. The material behavior for aluminium work piece is assumed as that of a Bingham fluid [11]. Tool and back plate are given thermal and fluid properties to carry out said thermo-fluid coupled analysis. But the important points to note here are that for tool and back plate the critical stress value and viscosities are set at very high values to proximate these components as virtual-solid fluids and the limitation exists for the used version of MSC Marc® to incorporate critical stress value for Bingham model as a function of temperature [9].

In MSC Marc® the method of weighted residuals is used to solve the coupled Navier-Stokes equations. Based upon conservation laws of momentum (mass and energy) the following first order differential equations are solved [9].

$$M\dot{v} + A(v)v + K(T,v)v - C_p + B(T)T = F(t) \qquad (1)$$

$$C^T v = 0 \qquad (2)$$

$$N\dot{T} + D(v)T + L(T)T = Q(v,t) \qquad (3)$$

In the above equations the notations for matrices are as under:

M	mass
A	advection of Momentum
K	viscosity matrix
B	buoyancy
F	external force
C^T	divergence matrix
N	heat capacitance
D	advection of energy
L	conductance matrix
Q	external flux
t	time
T	temperature
v	velocity
$\dot{}$	time rates
C_P	specific heat capacity

If the shear strain rate tensor is defined as:

$$\varepsilon_{ij} = \frac{1}{2}\left(\frac{\partial v_i}{\partial x_j} + \frac{\partial v_j}{\partial x_i}\right) \qquad (4)$$

and for viscous incompressible fluid the expression for deviatoric flow stress σ_{ij}^d using dynamic viscosity μ is given by:

$$\sigma_{ij}^d = 2\mu\dot{\varepsilon}_{ij} = \mu\dot{\gamma}_{ij} \qquad (5)$$

then the Bingham Fluid in MSC Marc® is represented as:

$$\sigma_{ij}^d = \mu_\circ \dot{\gamma}_{ij} + g\dot{\gamma}_{ij} \quad \text{if } \bar{\sigma} \geq g \qquad (6)$$

$$\dot{\gamma}_{ij} = 0 \quad \text{if } \bar{\sigma} < g \qquad (7)$$

Where,

$\dot{\gamma}_{ij}$ = strain rate

g = critical value of stress for at which the material starts the fluid behavior

The examples for the materials that can be modeled using Bingham Fluids include cement, slurries and pastes etc [9].
For the model eight nodded arbitrary hexahedral 3-D elements were used for meshing the tool, work piece and back plate. Due to tri-linear interpolation, with in these elements the strains tend to be constant and hence shear behavior is relatively rough, but at this stage the computational ease is preferred. Each model of all three tool geometries had approximately 8000 elements in its three dimensional mesh.
The material properties for the work piece are summarized in Table 03. The viscosity of the material during CFD analysis for FSW process is still a challenge and different constitutive relations are used in the literature, for example Seller-Tegart Law [1, 8] and Johnson-Cook Law [2]. However in this comparative study the simplified assumed viscosity below solidus temperature range is incorporated (i.e. 1.5 – 5 cP). Conductivities and heat capacities for all three components of the model i.e. tool, work piece and back plate, are incorporated as temperature dependant, these properties are given in [10].
Boundary Conditions: The temperatures at the tool top and back plate bottom are kept constant at ambient temperatures. The convection heat losses at tool and work piece outer surfaces are incorporated in the model. Variable fluid velocities with respect to radius of the tool keeping the sticking condition at tool–work piece interface are incorporated using user subroutines. The flow chart for the subroutines is shown in Figure 07.

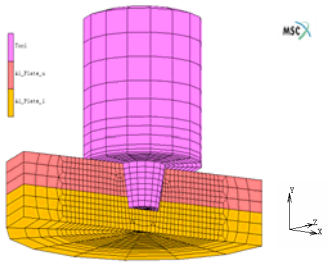

Figure 06: Mesh generated for the models of tool -2 and tool -3 (tools, aluminum sheets upper & lower)

The heat input is based upon so called engineering approach i.e. keeping the maximum temperatures below melting point of work piece. The heat distribution at tool surface has been incorporated with respect to contact area between tool and work piece.
Principally two load cases were defined for dwell and cooling phase with different time resolution. An additional load case was defined with coarse time resolution for extended phase of the Dwell to have better computational efficiency.

Results

The nugget size and shape in terms of velocity profile are the parameters being analyzed in this part of work. At this preliminary stage of current model the simple criteria for nugget (stirred zone) size and shape is set at a certain velocity to be sure about the stirring of the material at these values (i.e. around 12 mm/s). That corresponds to the velocity causing one complete revolution of the sheet material during the minimum dwell time, i.e. 1 second.

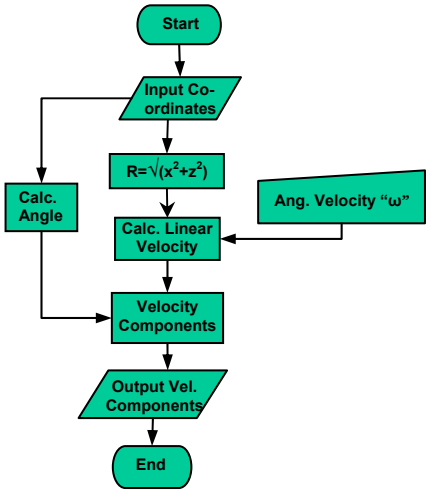

Figure 07: User subroutines flow chart for velocity variations at tool-work piece interface

Model Results: The model in this study, gave fluid and thermal outputs in terms of velocity and temperature profiles. The important results to analyze the material behavior for its flow were the nugget shape and size. For this, a planar view of velocity profile at point (0,0,0) normal to [0,0,1] was taken from the model output. The fluid zone was marked corresponding to limiting velocity stated above. Then the distance to the tool centre is plotted as function of pin length (figures 8 and 9).
Different simulated dwell times caused no change in the size and shape of the nugget as shown in figure 08. Though, off course the temperatures were risen due to extra energy input during the extended dwells.

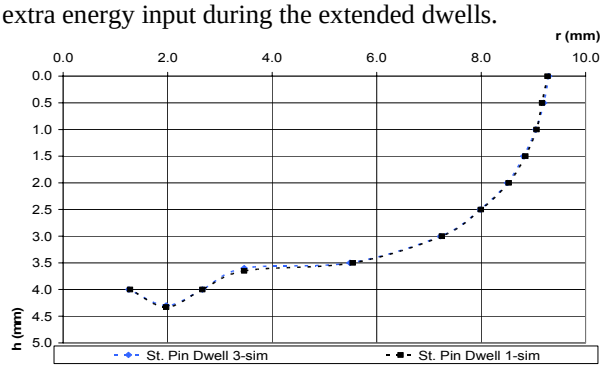

Figure 08: Dwell time (1 & 3 sec) effects for tool-2 at 1200 rpm as simulated

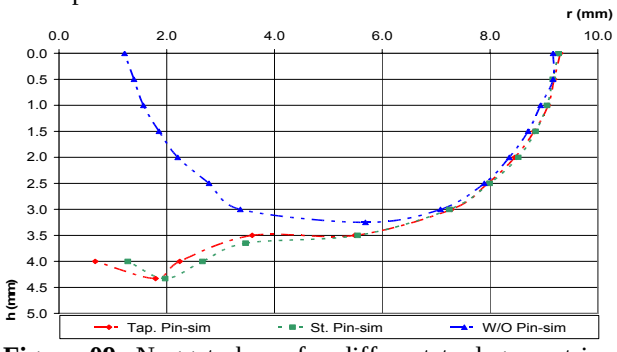

Figure 09: Nugget shape for different tool geometries as predicted by the model for rpm-dwell: 1200-1

For the effects of different rotational speeds the model shows a nugget size change due to higher velocities associated with higher rpm, but no change was shown in the shape of the nugget.

Another observation for model results is, that the effect of varying tool geometries, keeping rotational speed and dwell time constant, is not significant. The differences in nugget shape and size for three tools are present for tool-1 relative to tool-2 & 3 as in figure 9. The major difference is the presence of pin in lateral tool profiles. The difference between tool-2 and tool-3 is not prominent i.e. model is not predicting the pin-shape effect on the material behavior and hence on the flow.

Experimental Results: The experimental observations are made for all the above stated parameters i.e. tool geometry, rotational speed and dwell time. For the experimental results the cross section at the middle of the weld was captured to view the nugget shape and size (Figure 10). On the bases of grain size difference viewed at a constant magnification, the size and shape of stirred zone, identified as smallest equiaxed grains, was marked.

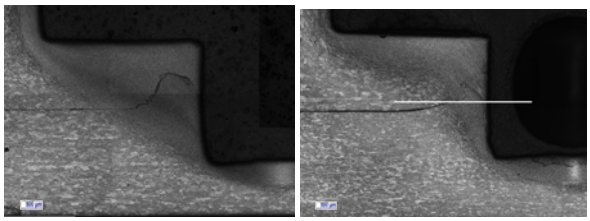

Figure 10: Experimental results for tool-2 at RPM-Dwell time of 800-0 and 1200-5 (left to right)

Variation in dwell times did not yield any considerable changes in terms of nugget shape and size for all the tools. A particular result for tool-2, at 1200 rpm and dwell times of 0, 1 & 5 seconds is shown in figure 11.

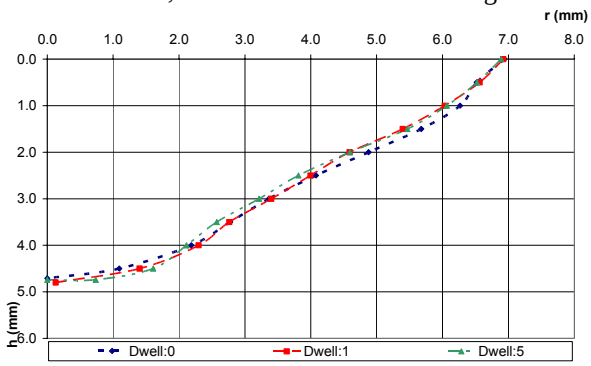

Figure11: Dwell time (0, 1 and 5 sec) effect on nugget shape & size for tool-2 at 1200 rpm

An interesting observation is made for tool-1 and tool-2 when the rotational speeds are varied. With increase of rotational speed, the nugget size reduces as shown in figure 12, whereas, this effect is not observed, for tool-3 as shown in figure 13.

Discussion

The model predicted a nugget which was relatively wider and deeper than the dimensions observed in the experimental results, for all three tools as shown in figure 9. The reason for this result may be due to relatively low viscosity difference in the model at extreme temperatures. The maximum possible range of viscosities could not be incorporated for the reason of stability of the calculations as higher velocities due to very low viscosities at the (virtual) solid – fluid interface are not supported by the FEA software package used for this study [9]. This limitation along with temperature independent critical yield strength for Bingham fluids in the used version of MSC Marc®, revealed the major short-coming of this model.

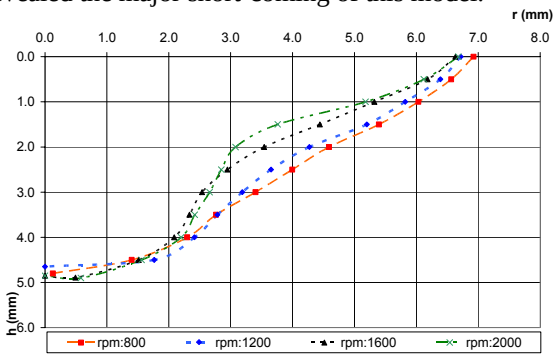

Figure 12: Effect of rotational speed for tool-2 at 1 sec dwell time

The shape of the nugget is hence dictated by variable velocity with respect to radius of the tool and viscosity difference due to temperature dependency and model could not sense the change in critical shear yield strength due to varying temperature profile in the work piece.

Though the dwell time effects predicted by the model are similar to experimental results i.e. very little or no change in nugget shape and size (figure 08), but the reason for this result by the model is that the effects on the material behavior which are dependant upon varying yield strength with respect to energy are not incorporated. Therefore the size and shape of the nugget from model results are not in agreement with the experimentally observed one.

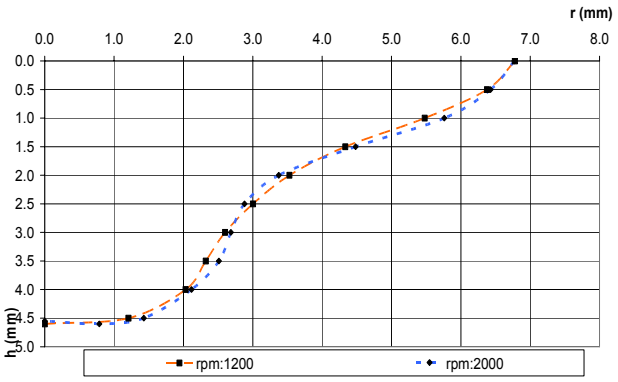

Figure 13: Effect of rotational speed for tool-3 at 1 sec dwell time

For the model results to study the effects of different rotational speeds the model showed the nugget size change due to higher velocities only. The possible improvement may be the incorporation of yield strength changes with respect to energy input.

For no considerable effect on the nugget shape and size by the variation of dwell time, as observed in the experimental results (figure 11), the possible reason could be that the nugget shape is already determined by the energy and its input rate during the plunge phase. The energy input during the dwell may be dictating the properties of the TMAZ and HAZ but not the nugget shape and size itself, as observed during this part of study.

The experimental observation for the effects of rotational speed on nugget shape and size (figure 12)

may lead to suggest an interesting hypothesis that when the energy is introduced to the work piece at higher rates the temperature gradient becomes steeper resulting in a steeper gradient for yield strength under the tool, as the yield strength is temperature dependant, shown in table 03 [10].

Table 03: Material properties of work piece (Al6082-T6)

Temperature (K)	Thermal Conductivity ($W.m^{-1}.K^{-1}$)	Sp. Heat Capacity ($J.kg^{-1}.K^{-1}$)	Tech. Yield Pt. (MPa)
293	215	885	61
373	212	915	55
473	215	952	41
573	216	992	33
673	208	1032	30
773	202	1073	20
873	196	1113	-

Hence the layers adjacent to tool – work piece interface region, which is the source of energy input from friction and deformation of material at the start of the process, become softer. The evidence for this may be observed in figure 14 by comparing the force required to plunge into the material i.e. forge force (kN).
So, at higher energy input rates, steeper temperature and yield strength gradient lead to thinner layers of material in the vicinity of tool – work piece interface, which can transmit the flow stresses to adjacent material layers, as the "slip" will occur between softer and the harder layers. The important point to note here is that the term softer layer is referred to the band of material with lower yield strength and viscosity ranges. The criteria for discretization of these ranges may be an interesting point for further study but are not investigated yet in the current project.

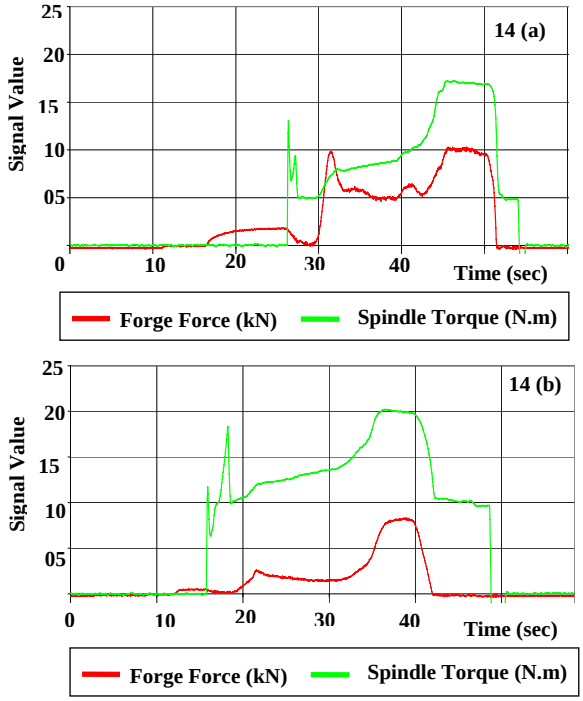

Figure 14: (a) Torque and forge force for tool-2 at 800-01 RPM-Dwell time (sec), (b) for 1200-01 RPM-Dwell time (sec)

In our study the observed results of tool-3, also provide a hint of support to this hypothesis i.e. effects of energy input amount and its rate on the nugget or stirred zone final size and shape. Due to tapered pin the penetration of the tool is facilitated and hence the low energy is required at the start of plunge and the gradual increase in the pin diameter also dictates a gradual energy input into the work piece, resulting in minimal effects on the final nugget shape.

Conclusions and Out Look

In this reported part of our study, the dwell time has minimal or no effects on the final nugget size and shape. The variation in rotational speed showed interesting effects, i.e. reduced nugget size at higher values of rotational speed for tool-1 & 2. Whereas for tool-3, this effect was not prominent, but owing to the tapered pin profile of the tool, it some how supported the hypothesis about the development of layered material behavior. The material behavior showed a strong relationship between yield strength changes, amount of energy input and its gradient, as the current simple model without this material characteristics was unable to accurately capture the experimentally observed nugget shape and size.
These observations from the experiments and model suggest further investigations for developing a relationship for discretization of material layers based upon varying yield strength with respect to energy input amounts and their rates. From modeling stand point, FE based model is working and at this stage serves as a platform to incorporate further details for the material behavior. That would lead to developing the criteria for change in yield strength as function of temperature. The variation in the assumed viscosity for Bingham fluid may be refined as well.

Acknowledgements

The financial support was given by Federal Ministry of Economy and Labor, Austria for this ongoing work on FSW. S. Khosa acknowledges the scholarship provided by Higher Education Commission (HEC) of Pakistan, managed by ÖAD Austria.

References:

[1] T. SEIDEL, A. REYNOLDS; Two-Dimensional FSW Process Model Based on Fluid Mechanics, Sc. & Tech. of Welding & Joining, Vol-8/3, 2003
[2] H. SCHMIDT, J. HATTEL; A local model for the thermo-mechanical conditions in FSW, Modelling Simul. Mater. Sci. Eng. 13 (2005) 77-93
[3] R. MISHRA, Z. MA; "Friction Stir Welding and Processing", Mater. Sc. and Engg. R 50 (2005) 1-78
[4] C. CHEN, R. KOVACEVIC; Thermo-Mechanical Modeling and force analysis of FSW by FEA, J. Mech. Engg. Sc. Vol.-218-C, 2004
[5] H. SHERCLIFF, P. COLEGROVE; "Modelling of Friction Stir Welding", Mathematical Modeling of Weld Phenomena–Volume VI, IWS-TU Graz (2005)
[6] M. AWANG et al.; Thermo-mechanical modeling of FSSW Process, SAE International 2005-01-1251
[7] N. MANDAL; "Aluminum Welding"2-ed. Asm Intl. 2006
[8] A. REYNOLDS; "Process Simulation in Friction Stir Welding", 8th International Seminar on Numerical Analysis of Weldability, Seggau-Graz (2006)
[9] MSC Marc® user manual Vol.-A; "Theory and user information", 2005
[10] P. TASIC; "Predictions of temperature fields in work piece and tool during FSSW by using FEA", Diploma Thesis, IWS – TU Graz, 2006
[11] W. HUJHES, J. BRIGHTON, "Fluid Dynamics" 3-ed, Schaum's Series-McGraw Hill, 1999